Scientific Research Publishing

Advances in Remote Sensing, 2025, 14(3), 188-205
https://www.scirp.org/journal/ars
ISSN Online: 2169-2688
ISSN Print: 2169-267X

Integrated Assessment and Mapping of Soil Water Erosion in a Tropical Urban Catchment Using Google Earth Engine: A Case Study of the Gourou Watershed (Abidjan, Côte d'Ivoire)

Kouamé Elyass Kanga[1*], Kouakou Hervé Kouassi[2], Kouakou Jean-Claude Tanoh[2], Yao Emile Desmond Konan[2], Arthur Brice Konan-Waidhet[2]

[1]Computer Science Laboratory, Environmental Science and Technology Laboratory, Department of Mathematics, Physics and Chemistry, Université Jean Lorougnon Guédé, Daloa, Côte d'Ivoire
[2]Environmental Science and Technology Laboratory, Department of Earth Sciences, Université Jean Lorougnon Guédé, Daloa, Côte d'Ivoire

Email: *elyass.kouame@gmail.com, kh.kouassi@gmail.com, jckouakou16@gmail.com, kyemiledes@gmail.com, konanwab@yahoo.fr2

How to cite this paper: Kanga, K.E., Kouassi, K.H., Tanoh, K.J.-C., Konan, Y.E.D. and Konan-Waidhet, A.B. (2025) Integrated Assessment and Mapping of Soil Water Erosion in a Tropical Urban Catchment Using Google Earth Engine: A Case Study of the Gourou Watershed (Abidjan, Côte d'Ivoire). *Advances in Remote Sensing*, **14**, 188-205.
https://doi.org/10.4236/ars.2025.143012

Received: August 13, 2025
Accepted: September 25, 2025
Published: September 28, 2025

Abstract

Water erosion constitutes a major threat to soil sustainability in tropical urban catchments exposed to intense rainfall and rapid urban expansion. This study assesses and maps soil loss in the Gourou watershed (Abidjan, Côte d'Ivoire) using the Revised Universal Soil Loss Equation (RUSLE) model implemented within the Google Earth Engine (GEE) platform. The methodological approach integrates multi-source data, including remote sensing products, *in situ* measurements (particle size analyses, permeability tests), and advanced spatial processing, to model the five RUSLE factors: rainfall erosivity (R), soil erodibility (K), topography (LS), land cover (C), and conservation practices (P). Results indicate an average annual soil loss of 50.20 t/ha/year—five times the tolerable threshold—and a total estimated loss of 132,286 tonnes/year. Erosion is exacerbated by high climatic erosivity (R: 950 - 1055 MJ·mm·ha^{-1}·h^{-1}·year^{-1}), locally fragile soils (K up to 0.452), steep slopes (LS > 8), and dense urbanization (66.77% of the watershed). Critical erosion zones (>359 t/ha/year), concentrated in the southern and eastern sectors, result from the combined effects of steep terrain, highly erodible soils, and impervious surfaces. These findings highlight the effectiveness of the RUSLE-GEE approach for rapid, accurate, and reproducible erosion assessment in tropical urban environments.

Keywords

Water Erosion, Spatial Modeling, Google Earth Engine (GEE), Remote Sensing, Geographic Information Systems (GIS), RUSLE Factors

1. Introduction

Soil water erosion represents one of the primary processes of environmental degradation in tropical regions, adversely affecting agricultural productivity, ecosystem stability, and the quality of water resources [1] [2]. In urban watersheds, this phenomenon is exacerbated by soil sealing, deforestation, and rapid land use changes, which promote increased surface runoff and heighten flood risks [3].

In West Africa, demographic pressure and unplanned urbanization have led to uncontrolled expansion of built-up areas, often at the expense of vegetation, thereby increasing soil vulnerability to erosion [4]. Urban watersheds in humid tropical zones display complex hydro-sedimentary dynamics, where the spatial variability of rainfall, topography, soil properties, and vegetation cover interactively influence soil loss rates [5].

The Gourou watershed, located within the city of Abidjan (Côte d'Ivoire), exemplifies these challenges. The area experiences a humid tropical climate with intense seasonal rainfall and rapid urban expansion, resulting in recurrent erosion, sedimentation, and flooding events that significantly impact the population, infrastructure, and surface water quality. Despite its strategic importance, few integrated studies have quantified and spatially mapped water erosion in this tropical urban context.

Traditionally, erosion assessment has relied on time-consuming and costly field measurements or models requiring site-specific data, which are often scarce in developing regions [6]. The emergence of high-resolution satellite imagery and cloud-based processing platforms such as Google Earth Engine (GEE) has opened new avenues for analyzing erosion processes at appropriate spatial and temporal scales, while efficiently integrating diverse data sources.

This study aims to deliver an integrated mapping of water-induced soil erosion in a tropical urban watershed using the Universal Soil Loss Equation (USLE) and multisource datasets processed via GEE. Applied to the Gourou watershed, the analysis seeks to enhance understanding of the spatial distribution of soil loss and provide a decision-support tool for sustainable resource management, urban planning, and especially the mitigation of flood risks.

2. Study Area

The Gourou watershed is located in the Autonomous District of Abidjan (Côte d'Ivoire). It lies between latitudes 5˚10' and 5˚25' North and longitudes 3˚59'10" and 4˚2'30" West. This watershed covers an area of approximately 27.5 km^2 [7], extending along a north-south axis about 9 km in length and 3 km in width from east to west. It is bounded to the east by the Boulevard Latrille, to the west by the Adjamé–Anyama railway line, to the north by the municipality of Abobo, and to the south by the Bay of Cocody and the Plateau municipality [8]. Its main drainage canal corresponds to the former bed of the "Gougou" river, as named in the Atchan (Ébrié) language. All surface water within the watershed converges toward its outlet located at the Indénié junction, at the intersection of the municipalities of Plateau, Cocody, and Adjamé, before flowing into the Ébrié Lagoon [8] (**Figure 1**).

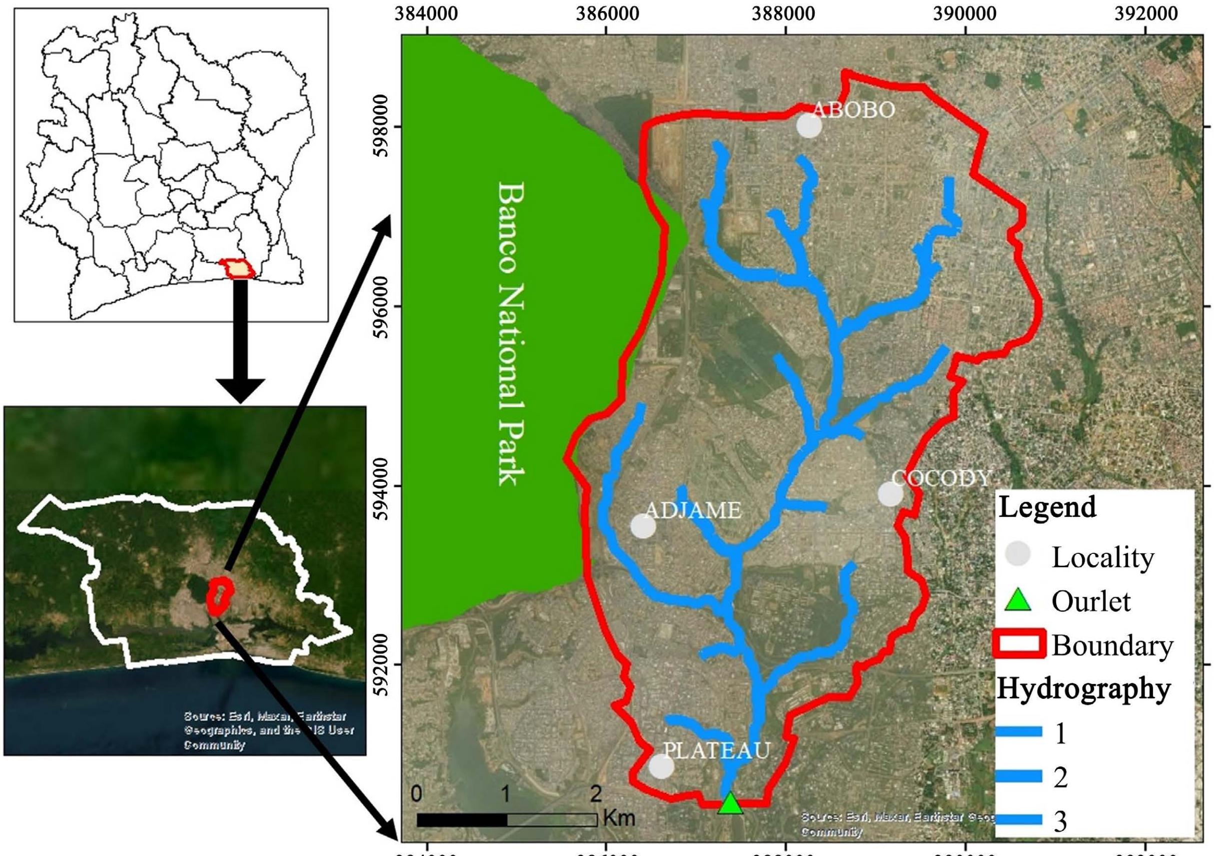

Figure 1. Gourou watershed extract from the administrative map of Abidjan from the Center for Cartography and Remote Sensing and placed on a Google Earth background.

3. Materials and Methods

3.1. Materials

The materials used for this study include both auxiliary datasets (**Table 1**) and software tools. The auxiliary data consist of a Landsat 8 OLI/TIRS image acquired on January 20, 2022 from the USGS EarthExplorer platform [9], a 12.5 m resolution Digital Elevation Model (DEM) from the ALOS PALSAR sensor [10], soil data collected during a field campaign in the study area, and climatic data derived from the CHIRPS rainfall database [11]. The Landsat image was processed using ENVI 5.3 software [12], while ArcGIS 10.8 [13] was employed for spatial analysis and geographic information system (GIS) operations.

Table 1. Sources and characteristics of input datasets used for hydrological erosion modeling in the Gourou watershed.

Data type	Associated factor	Format	Scale/Pixel Size	Data source
SRTM (DEM)	LS (Slope and length)	Raster (Géo Tif)	12.5 m	ALOS PALSAR https://search.asf.alaska.edu
Climate (Rainfall-CHIRPS)	R (Rainfall erosivity)	Raster (ESRI grids)	0.05˚ approx. 5 km	CHIRPS https://www.chc.ucsb.edu/data/chirps
Soil data (permeability, texture, organic matter)	K (Soil erodibility)	CSV	-	Field survey
Landsat 8 (Jan. 20, 2022)	C (Land cover factor)	Raster	30 m	USGS http://earthexplorer.usgs.gov

A Garmin GPSMAP 62x device [14] was used during the field survey to collect geographic coordinates of sampling locations.

Additionally, the Google Earth Engine (GEE) platform [15] was employed for the extraction and processing of climatic, pedological, and topographic data, as well as for the computation of the Universal Soil Loss Equation (USLE) factors (R, K, LS, C, and P). GEE is a cloud-based geospatial processing platform developed by Google, designed for large-scale environmental data analysis. It provides free access to an extensive catalog of satellite imagery (e.g., Landsat, Sentinel, MODIS) and climate datasets. The platform offers powerful tools for data processing, visualization, and spatial analysis, accessible through JavaScript or Python APIs.

One of GEE's main advantages is its ability to handle massive geospatial datasets efficiently, without requiring high-performance local computing resources. It enables access to both historical archives and near real-time data, making it particularly suited for environmental monitoring, land use/land cover change detection, forest monitoring, erosion mapping, flood assessment, and other Earth system science applications [16] [17].

3.2. Methods

The study of water-induced soil erosion in the Gourou watershed was conducted through a multi-criteria analysis integrating the factors of the Universal Soil Loss Equation (USLE). The methodological framework combined *in situ* measurements (permeability tests, soil sampling), digital processing (Google Earth Engine platform, Geographic Information Systems, and remote sensing), and spatial modeling techniques [15].

3.2.1. Rainfall Erosivity (R Factor)

Rainfall erosivity (R), a key component of the USLE model, was estimated using precipitation data from the CHIRPS (Climate Hazards Group InfraRed Precipitation with Stations) database [16]. These datasets, accessed via the Google Earth Engine (GEE) platform, were filtered by temporal range and the area of interest (AOI) to compute the cumulative rainfall for the study period. The mean annual rainfall over the watershed was then derived and used to estimate rainfall erosivity using the simplified empirical formula proposed by Fenta *et al.* (2020) [18]:

$$R = 0.5 \times P_{annual} \quad (1)$$

R is the rainfall erosivity (MJ·mm·ha^{-1}·h^{-1}·yr^{-1}),

P_{annual} is the mean annual precipitation in millimeters (mm).

This simplified formulation is widely used in tropical regions of West Africa, where rainfall is characterized by high intensity and marked seasonal distribution. It is particularly suitable for the West African context as it adequately reflects the nonlinear relationship between annual rainfall and the kinetic energy of precipitation, as confirmed by Fenta *et al.* (2020) [18]. Its application thus enables a robust and regional estimation of the R factor, consistent with the climatic conditions of high rainfall intensity typical of the Gourou watershed.

3.2.2. Soil Erodibility (K Factor)

Soil erodibility (K) assesses the susceptibility of a soil to erosion based on its permeability, texture, structure, and organic matter content. In this study, the K factor was determined through *in situ* permeability tests and laboratory analyses. These measurements allowed for the application of the empirical formula proposed by Wischmeier & Smith [6]:

Soil erodibility (K) assesses the susceptibility of soil to erosion based on its permeability, texture, structure, and organic matter content ([16]). In this study, the K factor was determined through *in situ* permeability tests and laboratory analyses. These measurements allowed for the application of the empirical formula proposed by Wischmeier and Smith ([6]):

$$\mathrm{K} = 2.1 \times M^{1.14} \times 10^{-6} \left(12 - MO\right) + 0.0325 \times \left(b - 2\right) + 0.025 \times \left(C - 3\right) \tag{2}$$

where

- M represents the texture parameter, calculated as (%silt + %very fine sand) × (100 − %clay);
- MO is the organic matter content (%); b is the soil structure code (on a scale from 1 to 6);
- c is the permeability class (on a scale from 1 to 6).

Permeability tests were conducted at 19 locations across the watershed, limited by access constraints due to urban development. These observations provided a spatially representative basis for estimating K values across the study area (**Figure 2**, **Figure 3**).

Based on Porchet's method and the Beerkan infiltration theory [19], field tests were conducted during the dry season using an infiltrometer. Water was poured into boreholes between 30 and 100 cm deep to measure the infiltration rate, thereby assessing the soil's water absorption capacity and susceptibility to surface runoff.

Soil samples were collected at 19 georeferenced locations across the watershed, at depths ranging from 30 to 100 cm, using manual augers. Each sample, weighing approximately 500 g, was taken from homogeneous soil profiles located near visible erosion features (e.g., gullies or rills). Particle size analysis was performed at the CRE laboratory (Université Nangui Abrogoua) following the AFNOR NF X31-107.500 [20] standard, to determine the relative proportions of sand, silt, and clay. These textural data, combined with permeability measurements, were used to evaluate the soil's susceptibility to water erosion. The K-factor map was generated on Google Earth Engine using Inverse Distance Weighting (IDW) interpolation from the georeferenced sample points.

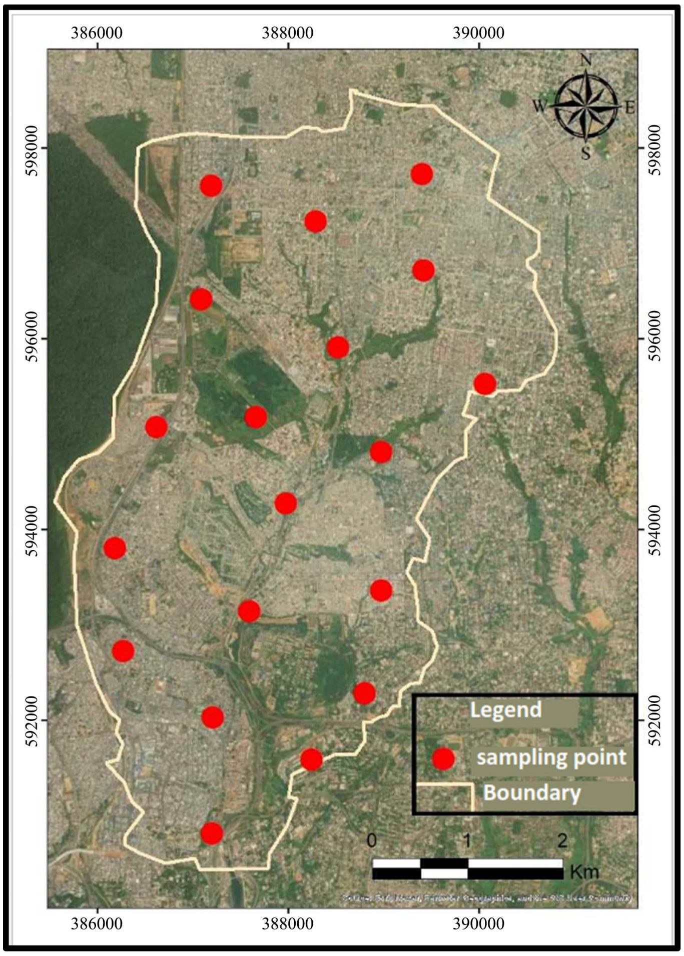

Figure 2. Sampling points selected (Sampling point interpolated from ArcMap and placed on a Google Earth background).

Figure 3. Infiltrometer test at Cocody.

3.2.3. Slope Gradient (LS Factor)

As part of the assessment of water-induced soil erosion in the Gourou watershed, the LS factor (slope length (λ) × slope steepness (θ)) [21] was computed using the Google Earth Engine (GEE) platform from a Digital Elevation Model (DEM). The DEM was first processed with a focal mean filter to reduce irregularities and improve flow direction calculations [22]. The slope gradient was derived from the smoothed DEM and then converted to radians in order to compute the tangent of the slope angle ($\tan\theta$), which is required for calculating the LS factor [22]. The slope length (λ) was estimated from the flow accumulation derived from the filtered DEM, with values constrained between 10 and 100 meters to remain within realistic hydrological thresholds [23]. The LS factor was then computed by combining two components [22]:

$$LS_\lambda = \left(\frac{\lambda}{22.13}\right)^{0.9} \tag{3}$$

$$LS_\theta = \left(\frac{\tan\theta}{0.0896}\right)^{1.3} \tag{4}$$

3.2.4. Land Use/Land (C Factor)

The C factor, representing the impact of vegetation cover on soil erosion, was estimated using a land use/land cover (LULC) map derived from a 2022 Landsat image. This map was generated through supervised classification using the maximum likelihood algorithm in ENVI software, and subsequently validated through a field survey [24].

Four main land cover classes were identified:

- Built-up/Bare soil,
- Dense forest,
- Degraded forest,
- Wetlands/Croplands.

Each class was assigned a C value according to the reference values established by Wischmeier and Smith [6] and refined by Lufafa *et al.* [24] (**Table 2**). The C factor map was subsequently produced in Google Earth Engine by rasterizing the classified LULC data and reclassifying each pixel according to its corresponding C value.

Table 2. Land use classes and corresponding C-factor (Cover-Management Factor) values [6] [24].

Class	Land use	C Facteur Range
1	Dense forest	0.001 - 0.01
2	Degraded forest	0.01 - 0.05
3	Wetland/Cropland	0.2
4	Urban area	0.15 - 0.25
5	Bare soil	0.5 - 1

3.2.5. Soil Conservation Practices (P Factor)

The support practice factor (P) is a key parameter in assessing soil water erosion, as it quantifies the effectiveness of soil conservation measures in reducing soil loss. To determine this factor, field data on existing conservation practices were collected, including the presence of terraces, vegetative buffer strips, and contour farming. However, due to the high degree of urbanization in the Gourou watershed, no structured soil conservation practices were observed. Moreover, on the remaining permeable land areas (agricultural or natural zones), no artificial soil conservation techniques—such as terracing, benching, or contour plowing—are implemented. Therefore, the P factor is set to 1 across the entire watershed. This value reflects the absence of effective mechanical or agronomic conservation practices. It is important to note that while the C factor (cover and management factor) already accounts for land cover effects—including vegetation cover and impervious surfaces (e.g., built-up areas)—the P factor specifically addresses deliberate conservation interventions aimed at controlling erosion. In this context, assigning P = 1 is fully justified, consistent with field observations and previous studies conducted in similar environments [25].

3.2.6. Integration of USLE Factors in Google Earth Engine (GEE)

The final USLE model was implemented in GEE, combining the R, K, LS, C, and P layers into a spatially distributed soil loss map:

$$A = R \times K \times LS \times C \times P \tag{5}$$

where A represents annual soil loss ($t \cdot ha^{-1} \cdot yr^{-1}$). This cloud-based workflow ensures computational efficiency, reproducibility, and integration of multi-source geospatial datasets [15] [16].

4. Results

4.1. Rainfall Erosivity (R Factor)

The R factor, expressed in $MJ \cdot mm \cdot ha^{-1} \cdot h^{-1} \cdot year^{-1}$, quantifies the climatic erosivity associated with precipitation. It reflects the rainfall's capacity to detach and transport soil particles as a function of its intensity and temporal distribution. Spatial analysis of the R factor shows values ranging from 950 to 1055 $MJ \cdot mm \cdot ha^{-1} \cdot h^{-1} \cdot year^{-1}$, with an average annual rainfall of 1976 mm. An uneven distribution of the R factor is observed across the Gourou watershed. In the northern sector, the R factor is lowest (around 950 $MJ \cdot mm \cdot ha^{-1} \cdot h^{-1} \cdot year^{-1}$), indicating slightly less intense or less temporally concentrated rainfall, and thus a relatively lower climatic erosion pressure. The central and southeastern areas display intermediate values (950 - 1010), corresponding to moderate to high erosivity, which can increase erosion susceptibility if soils are poorly protected. The southwestern and southern sectors record the highest values (>1010), reflecting high rainfall kinetic energy. These areas are particularly vulnerable to water erosion, especially where steep slopes or highly erodible soils are present (**Figure 4**).

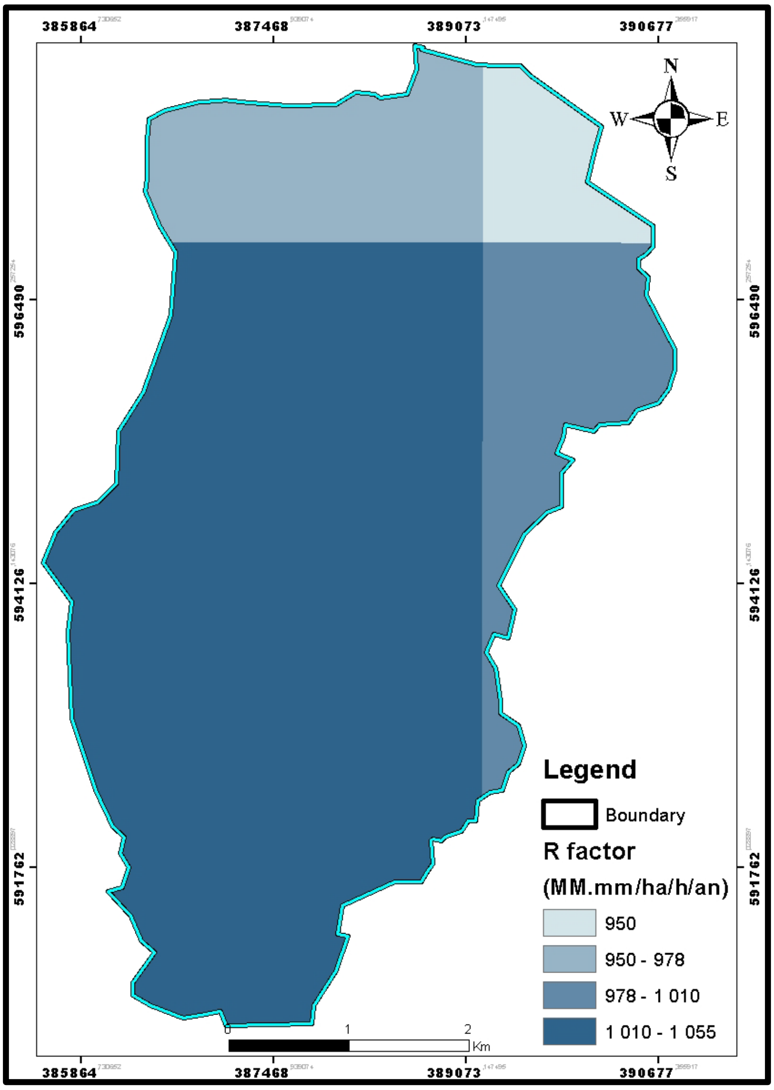

Figure 4. Rainfall erosivity factor (R) in the Gourou Watershed.

4.2. Soil Erodibility (K Factor)

The K factor, representing soil erodibility, ranges from 0.015 to 0.452 across the Gourou watershed, spanning from low to high erodibility zones. This spatial distribution highlights marked contrasts in erosion susceptibility, directly linked to soil texture, structure, organic matter content, and aggregate stability.

Low erodibility areas (0.015 - 0.094), covering 47.37% of the watershed, are mainly concentrated in the central and northwestern sectors. These soils exhibit a high proportion of clay and/or organic matter, which enhances cohesion and resistance to detachment by raindrop impact. Such areas play a protective role against water erosion, even under high rainfall conditions.

Moderate erodibility zones (0.094 - 0.222), accounting for 36.84% of the watershed, are found predominantly in the mid-western portion. These soils are generally loamy-sand in texture, making them more susceptible to detachment while retaining a certain degree of resistance due to stable soil structure.

Finally, high erodibility areas (0.222 - 0.452), primarily located in the north-central, southern, southwestern, and southeastern sectors, correspond to lighter soils (rich in silt and fine sand), low in organic matter, and with poor structural stability. Such properties promote rapid particle detachment. These zones, which represent 15.79% of the watershed, constitute critical hotspots where erosion risk is particularly high (Figure 5).

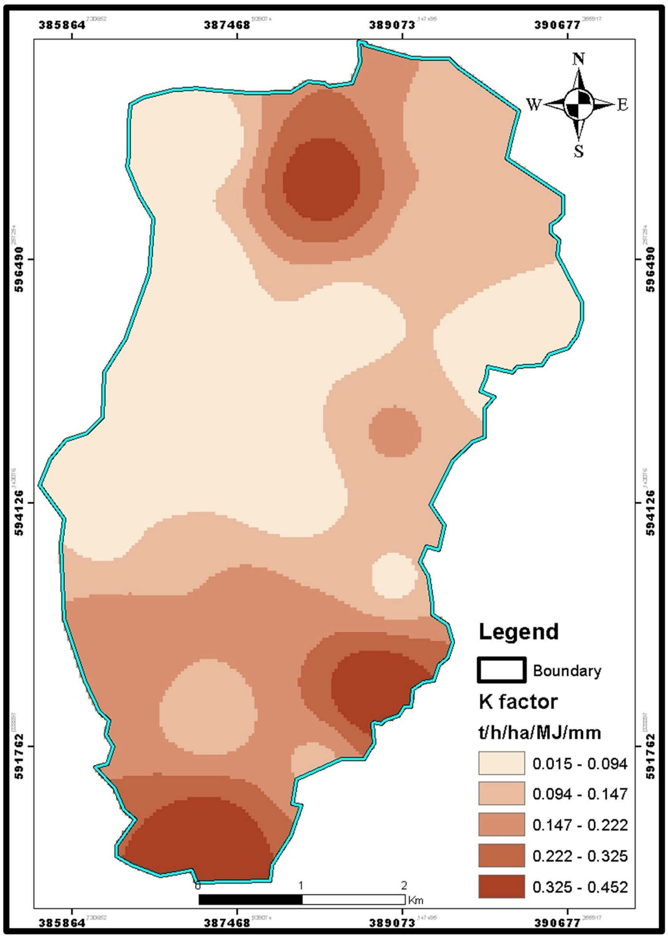

Figure 5. Spatial interpolation of the soil erodibility factor (K) based on field measurements.

4.3. Slope Gradient (LS Factor)

The LS factor values in the Gourou watershed range from 0 to 8.32, with a mean value of 1.13. Classification of these values into four categories reveals a spatial variability in erosion risk according to slope gradient and flow length.

- Class 0 - 0.81: covers 43.36% of the area (1146.99 ha). These are areas characterized by gentle slopes and short flow lengths, exhibiting low susceptibility to soil erosion.
- Class 0.81 - 1.85: represents 25.90% (684.73 ha), with moderate slopes showing an increasing erosion risk, particularly under conditions of fragile soils or intense rainfall events.

- Class 1.85 - 3.39: encompasses 14.71% (388.63 ha), where steeper slopes promote rapid surface runoff, enhancing overland flow and erosion potential.
- Class 3.39 - 8.32: occupies 16.03% of the watershed (424.30 ha). These areas are the most vulnerable to water-induced erosion due to steep slopes and long runoff pathways.

This distribution highlights a clear contrast between flat lowland areas, which are less prone to erosion, and steeply sloped regions, where erosion risk is significantly elevated (Figure 6).

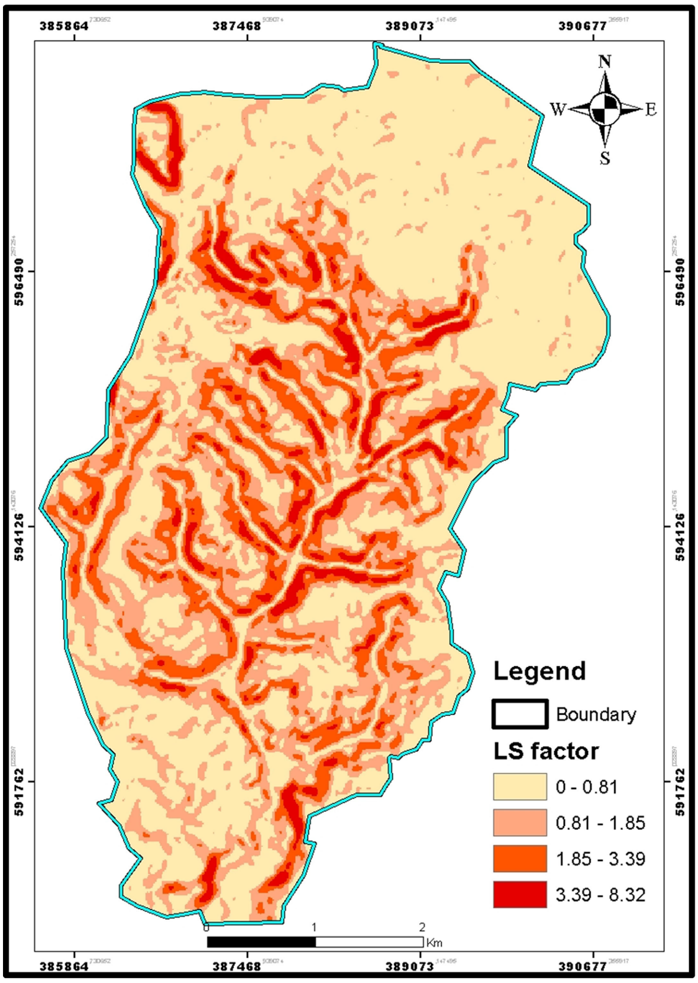

Figure 6. Topographic factor (LS) derived from slope gradient and flow accumulation using DEM data.

4.4. Land Use/Land (C Factor)

The assessment of the cover-management factor (C) highlights the influence of vegetation cover on erosion susceptibility within the Gourou watershed. Forested areas, including dense (0.001 - 0.01), and degraded forests (0.01 - 0.5), account for 19.22% of the study area, providing variable but generally low to moderate erosion protection depending on canopy density. Wetlands and agricultural lands (0.1 - 0.2) represent only 1.10% of the watershed and offer moderate protection against soil loss. In contrast, urban areas cover 66.77% of the surface and are associated with high C-factor values (0.15 - 0.25), promoting surface runoff and soil erosion due to extensive soil sealing and impervious surfaces. Bare soils, which are highly susceptible to erosion, constitute 12.91% of the area and exhibit the highest C-factor values (0.5 - 1.0), significantly contributing to soil loss.

Overall, 20.32% of the watershed exhibits low erodibility (forests, croplands), 66.77% shows moderate to high erodibility (urban areas), and 12.91% is classified as highly erodible (bare soils). This distribution underscores the dominant role of land cover, particularly urbanization and bare ground, in increasing the watershed's vulnerability to water erosion (**Figure 7**).

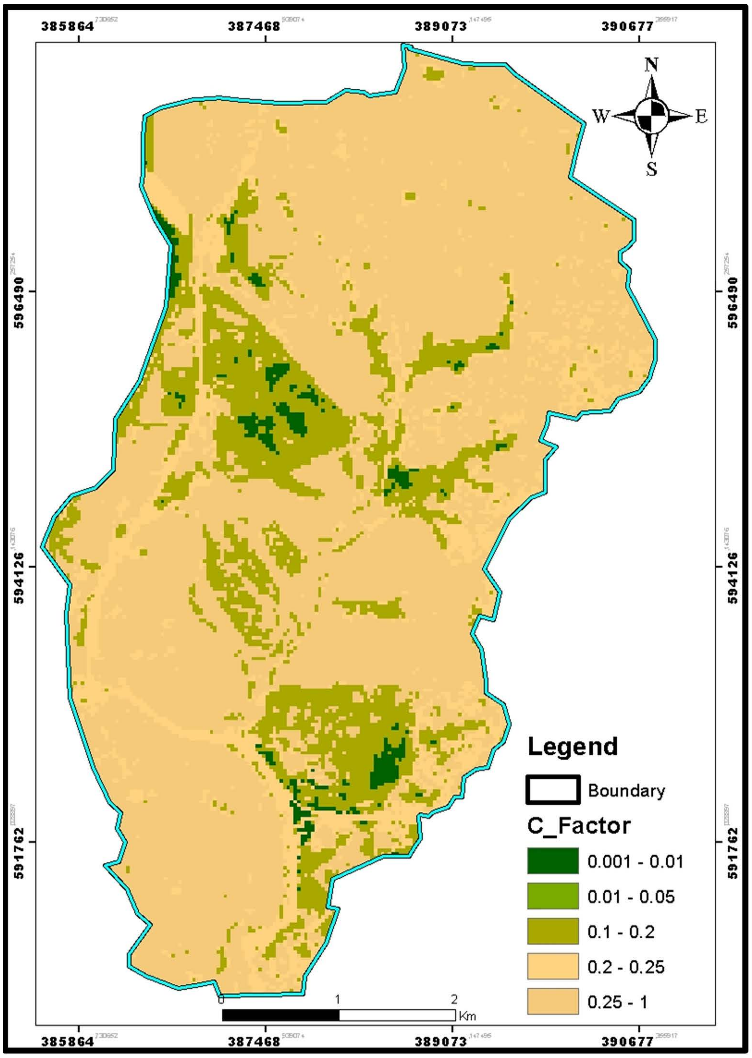

Figure 7. Land cover factor (C) derived from land use classification of Landsat imagery.

4.5. Soil Loss Estimation

The application of the RUSLE model, integrating the five factors (R, K, LS, C, P), enabled the estimation of soil losses across the Gourou watershed. Losses range from 0 to 1698 t/ha/year, with an alarming mean value of 50.20 t/ha/year—well above the tolerable threshold of 10 t/ha/year for urban environments as defined by the FAO. The total annual soil loss is estimated at 132,286.34 tonnes, highlighting a concerning level of erosion.

Most of the watershed is characterized by low to moderate soil loss values, predominantly between 0 and 146 t/ha/year (Table 3), covering over 90% of the study area (Figure 8).

Table 3. Distribution of soil loss in the Gourou watershed.

CLASS	Area (km^2)	Area (ha)	Percentage (%)	Average (t/ha/year)
Low loss (<46 t/ha/year)	19.13	1913.04	72.27	
Moderate loss (46 - 146 t/ha/year)	5.5	550.17	20.78	
High loss (146 - 359 t/ha/year)	1.47	147.13	5.55	50.20
Very high loss (359 - 739 t/ha/year)	0.21	20.83	0.79	
Extreme loss (739 - 1698 t/ha/year)	0.16	16.36	0.60	
Total	**26.48**	**2647.54**	**100.00**	

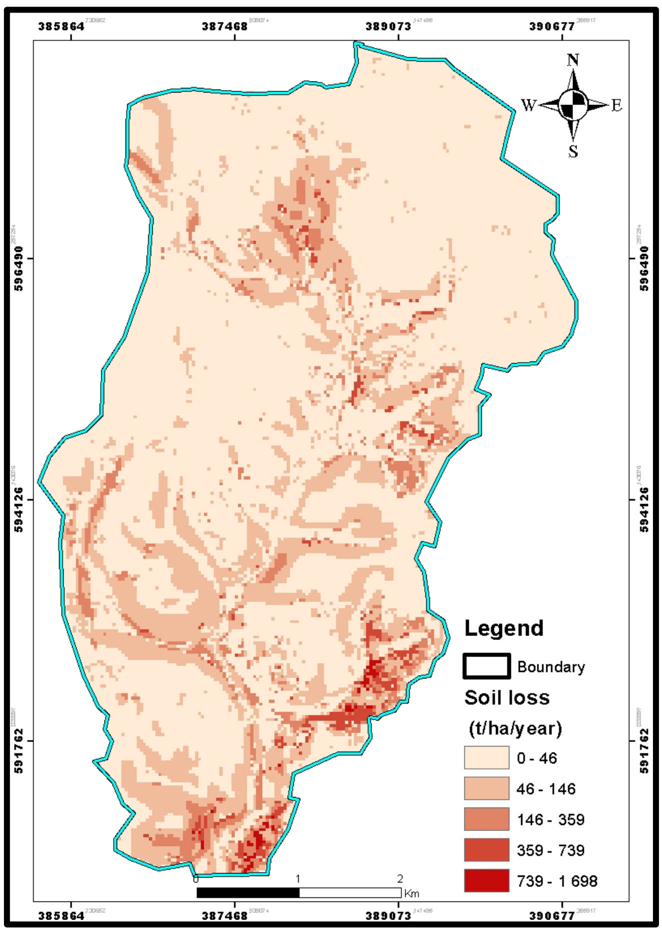

Figure 8. Soil loss mapping in the Gourou watershed.

This indicates diffuse but overall controlled erosion across the majority of the basin. High and very high erosion zones (A > 359 t/ha/year), covering 6.64% of the watershed, are concentrated in the southern sector, particularly near the outlet. Here, the combination of steep slopes, low vegetation cover, and erosion-prone soils (high K values) results in significant soil losses. A similar trend is observed in the eastern and northeastern sectors, driven by intense urbanization, surface imperviousness, and poorly managed artificial drainage systems.

5. Discussion

Integrated analysis of water-induced soil erosion in the Gourou watershed, conducted using the Revised Universal Soil Loss Equation (RUSLE) model and remote sensing tools via Google Earth Engine (GEE), reveals a critical situation regarding soil degradation, particularly exacerbated by rapid anthropogenic dynamics characteristic of tropical urban environments. This discussion interprets the results by analyzing the biophysical factors (R, K, LS, C, P) and their spatial interactions, while contextualizing them within the environmental, climatic, and urban specificities of the watershed.

The spatialization of the R factor, ranging from 950 to 1055 $MJ \cdot mm \cdot ha^{-1} \cdot h^{-1} \cdot an^{-1}$, confirms the high kinetic energy of tropical rainfall, consistent with values reported in other coastal urban watersheds in West Africa. For instance, Koné *et al.* (2020) estimated R values between 900 and 1100 $MJ \cdot mm \cdot ha^{-1} \cdot h^{-1} \cdot an^{-1}$ in the Mé River basin (Côte d'Ivoire), highlighting the similarity of humid tropical rainfall regimes [26]. This high climatic erosivity underscores the critical importance of soil protection measures in such environments.

The K factor indicates that 15.79% of the watershed consists of highly erodible soils (K > 0.222), a proportion comparable to findings by Tapsoba *et al.* (2019) in Burkina Faso (14.5% of soils with high erodibility), although in a more semi-arid context [27]. The key difference lies in the fact that, in the Gourou watershed, high soil erodibility coincides with elevated rainfall erosivity (R), which significantly amplifies soil loss. However, the K factor map was interpolated from only 19 soil sampling points, which represents a potential source of spatial uncertainty; future studies could refine this estimate through a denser and more representative soil sampling across the watershed.

The LS factor reveals that 16.03% of the basin lies in steep terrain (LS > 3.39), aligning with observations by Zougmore *et al.* (2018) in Ghana, where urban areas with steep slopes exhibited soil losses up to three times higher than flat areas due to concentrated surface runoff [28].

The C factor highlights the decisive role of land cover: forest cover accounts for only 19.22% of the area, compared to over 50% in rural basins studied by Ouattara *et al.* (2017) [29] in central Côte d'Ivoire—partly explaining the significantly higher mean soil losses observed in this study. Urban areas, covering 66.77% of the watershed, enhance surface runoff by reducing infiltration, a phenomenon previously emphasized by Kouadio *et al.* (2021) in Abidjan, where surface sealing increased erosion by nearly 40% over less than two decades [30].

Soil loss estimation using the RUSLE model yields an alarming average loss of 50.20 t/ha/year, five times the tolerable limit of 10 t/ha/year established by the FAO [31]. This value exceeds average losses reported in other African urban basins (e.g., 18.6 t/ha/year in the Mefou basin, Cameroon; 22.5 t/ha/year in Abidjan), highlighting accelerated soil degradation in the Gourou watershed [32]. The total annual soil loss of 132,286.34 tonnes represents a significant potential for downstream sedimentation, with adverse impacts on river systems, reservoirs, and hydraulic infrastructure. While over 90% of the area experiences low to moderate erosion (0 - 146 t/ha/year), the 6.64% of areas with very high erosion (>359 t/ha/year)—located in the southern part near the outlet—constitute critical erosion hotspots where soil losses are severe and demand immediate mitigation.

6. Conclusions

The study on water-induced soil erosion in the Gourou watershed reveals accelerated soil degradation resulting from a critical combination of natural and anthropogenic factors. The findings indicate an average soil loss of 50.20 t/ha/year, five times the tolerable threshold of 10 t/ha/year established by the FAO, with localized peaks exceeding 1600 t/ha/year. This severe erosion, amounting to an annual total loss of 132,286 tons, is driven by high rainfall erosivity (R-factor: 950 - 1055 $MJ \cdot mm \cdot ha^{-1} \cdot h^{-1} \cdot year^{-1}$), inherently erodible soils (K-factor up to 0.452), steep slopes (LS-factor > 8), and—most critically—uncontrolled urban expansion, which dominates 66.77% of the area.

The near-disappearance of protective vegetation cover, soil sealing, and the prevalence of extensive bare soil zones (12.91%) exacerbate runoff and reduce infiltration, transforming the watershed into a system highly vulnerable to erosive processes. The most critical areas, located in the south, southwest, and near the outlet, highlight the detrimental synergy between topography, fragile soils, and urban pressure, generating extreme soil losses that threaten infrastructure stability, watercourse quality, and long-term soil resource sustainability.

This study demonstrates the effectiveness of the integrated RUSLE-Google Earth Engine approach for mapping and quantifying soil erosion at a large scale, offering high reproducibility and low operational cost. It calls for urgent and sustainable watershed management, but more importantly, for concrete and spatially targeted interventions grounded in the study's findings.

Indeed, the mapping of critical erosion zones (>359 t/ha/year) identifies priority areas for ecological restoration. Targeted revegetation of these zones—particularly through the planting of locally adapted, deep-rooted plant species such as Andropogon gayanus, Hyparrhenia rufa, and Chromolaena odorata—could stabilize soils, reduce surface runoff, and restore essential ecosystem protective functions. The establishment of grassed strips or windbreak hedges along slopes could further mitigate raindrop impact and slow down overland water flow.

In urbanized areas, where surface sealing dominates, the implementation of low-impact development (LID) practices for stormwater management emerges as an urgent solution. This includes the construction of permeable pavements, vegetated swales (bioswales), rain gardens, and retention basins designed to reduce both the volume and velocity of runoff. These proven techniques, already successfully applied in other tropical urban contexts, could be integrated into urban planning and informal settlement upgrading projects, particularly in sloping areas.

Furthermore, the absence of soil conservation practices (P = 1) underscores the need to incorporate erosion control measures into land-use and urban planning frameworks. This could be achieved through regulatory mechanisms such as restricting land development on steep slopes, prohibiting the exposure of bare soils, and promoting simple, low-cost techniques like contour plowing and the preservation of vegetated slope buffers.

Finally, local authorities and decision-makers should use this erosion map as a foundation for developing an integrated watershed management plan. Such a plan should include regular monitoring via remote sensing, community awareness campaigns, and incentives for the preservation of green spaces. Vegetated riparian buffer zones should be established along watercourses to reduce downstream sedimentation and protect hydraulic infrastructure.

Without rapid and targeted interventions, the Gourou watershed risks irreversible soil degradation, with severe long-term consequences for environmental, water, and food security. This study provides not only a precise diagnosis but also an operational roadmap for proactive, evidence-based management—essential for enhancing the ecological and urban resilience of the watershed.

Conflicts of Interest

The authors declare no conflicts of interest regarding the publication of this paper.

References

[1] Lal, R. (2001) Soil Degradation by Erosion. *Land Degradation & Development*, **12**, 519-539. https://doi.org/10.1002/ldr.472

[2] Morgan, R.P.C. (2005) Soil Erosion and Conservation. 3rd Edition, Blackwell Publishing.

[3] Boardman, J. and Poesen, J. (2006) Soil Erosion in Europe. In: Boardman, J. and Poesen, J., Eds., *Soil Erosion in Europe*, Wiley, Chichester, 479-487.

[4] Karambiri, H., Garba, I., Ouedraogo, M., Somé, L. and Koïta, M. (2011) Impacts of Climate Change and Human Activities on Hydrology of West African Sahel. *Journal of Hydrology*, **404**, 118-129.

[5] Food and Agriculture Organization (FAO) (2019) Soil Erosion: The Greatest Challenge for Sustainable Soil Management. FAO.

[6] Wischmeier, W.H. and Smith, D.D. (1978) Predicting Rainfall Erosion Losses: A Guide to Conservation Planning. USDA Agriculture Handbook No. 537. U.S. Government Printing Office.

[7] BRL (2015) Étude d'actualisation du Schéma Directeur d'Assainissement et de Drainage du District d'Abidjan. Rapport technique, Ministère des Infrastructures Économiques, Abidjan.

[8] Coulibaly, K.M., Kouamé, K.J. and N'Go, Y.A. (2011) Analyse des facteurs d'inonda-

tions dans la ville d'Abidjan: Cas du bassin versant du Gourou. *Revue de Géographie Tropicale et d'Environnement*, **1**, 69-84.

[9] USGS (2022) Landsat 8 OLI/TIRS Data Product. United States Geological Survey. https://earthexplorer.usgs.gov/

[10] JAXA (2022) ALOS PALSAR Digital Elevation Model (12.5 m). Japan Aerospace Exploration Agency. https://www.eorc.jaxa.jp/ALOS/en/aw3d30/

[11] Funk, C., Peterson, P., Landsfeld, M., Pedreros, D., Verdin, J., Shukla, S., *et al.* (2015) The Climate Hazards Infrared Precipitation with Stations—A New Environmental Record for Monitoring Extremes. *Scientific Data*, **2**, Article No. 150066. https://doi.org/10.1038/sdata.2015.66

[12] Harris Geospatial Solutions (2020). ENVI 5.3 User Guide. https://www.l3harrisgeospatial.com/Software-Technology/ENVI

[13] ESRI (2020) *ArcGIS Desktop 10.8.* Environmental Systems Research Institute.

[14] Garmin (2020) GPSMAP 62 Series Owner's Manual. Garmin Ltd. https://www.garmin.com

[15] Gorelick, N., Hancher, M., Dixon, M., Ilyushchenko, S., Thau, D. and Moore, R. (2017) Google Earth Engine: Planetary-Scale Geospatial Analysis for Everyone. *Remote Sensing of Environment*, **202**, 18-27. https://doi.org/10.1016/j.rse.2017.06.031

[16] Kumar, L. and Mutanga, O. (2018) Google Earth Engine Applications since Inception: Usage, Trends, and Potential. *Remote Sensing*, **10**, Article 1509. https://doi.org/10.3390/rs10101509

[17] Tamiminia, H., Salehi, B., Mahdianpari, M., Quackenbush, L., Adeli, S. and Brisco, B. (2020) Google Earth Engine for Geo-Big Data Applications: A Meta-Analysis and Systematic Review. *Journal of Photogrammetry and Remote Sensing*, **164**, 152-170. https://doi.org/10.1016/j.isprsjprs.2020.04.001

[18] Fenta, A.A., Yasuda, H., Shimizu, K., Haregeweyn, N., Kawai, T., Sultan, D., Ebabu, K., Belay, A.S., Mekonnen, M. and Mamo, G. (2020) Evaluation of the Revised Universal Soil Loss Equation (RUSLE) Under Different Rainfall and Land Use Conditions in the Upper Blue Nile Basin, Ethiopia. *Journal of Arid Environments*, **181**, Article 104231.

[19] Porchet, L., Fourrié, N., Lavenue, F., Boucard, A. and Laurent, F. (2013) Application de la loi d'infiltration de Beerkan en climat tropical: Étude de cas sur sols compacts. *Revue des Sciences de l'Eau*, **26**, 211-225.

[20] AFNOR (1995) Norme NF X31-107.500—Détermination de la distribution granulométrique des sols. Association Française de Normalisation. Decagon Devices Inc (2015) Mini Disk Infiltrometer User's Manual. Decagon Devices, Pullman, WA.

[21] Desmet, P.J.J. and Govers, G. (1996) A GIS Procedure for Automatically Calculating the USLE LS Factor on Topographically Complex Landscape Units. *Journal of Soil and Water Conservation*, **51**, 427-433. https://doi.org/10.1080/00224561.1996.12457102

[22] Moore, I.D. and Burch, G.J. (1986) Physical Basis of the Length-Slope Factor in the Universal Soil Loss Equation. *Soil Science Society of America Journal*, **50**, 1294-1298. https://doi.org/10.2136/sssaj1986.03615995005000050042x

[23] Van Remortel, R.D., Maichle, R.W. and Hickey, R.J. (2004) Computing the LS Factor for the Revised Universal Soil Loss Equation through Array-Based Slope Processing of Digital Elevation Data Using a C++ Executable. *Computers & Geosciences*, **30**, 1043-1053. https://doi.org/10.1016/j.cageo.2004.08.001

[24] Lufafa, A., Tenywa, M.M., Isabirye, M., Majaliwa, M.J.G. and Woomer, P.L. (2003)

Prediction of Soil Erosion in a Lake Victoria Basin Catchment Using a GIS-Based Universal Soil Loss Model. *Agricultural Systems*, **76**, 883-894. https://doi.org/10.1016/s0308-521x(02)00012-4

[25] N'go, Y.A. (2015) Évaluation de la vulnérabilité du bassin versant du Béoumi (centre de la Côte d'Ivoire) aux inondations urbaines: Approche multicritère. Thèse de Doctorat, Université Félix Houphouët-Boigny.

[26] Koné, B.W., Koffi, K.A., Kouamé, F.K. and Atsé, B.C. (2020) Assessment of Rainfall Erosivity and Soil Loss in the Mé River basin (Côte d'Ivoire) Using GIS and RUSLE Model. *Journal of Water Resource and Protection*, **12**, 533-550.

[27] Tapsoba, N., Kouame, K.F., Ouedraogo, M. and Barry, B. (2019) Soil Erosion Risk Assessment in the Mouhoun River basin (Burkina Faso) Using RUSLE Model and GIS. *International Soil and Water Conservation Research*, **7**, 244-252.

[28] Zougmore, R., Bationo, A. and Sedogo, M.P. (2018) Land Use Change and Soil Erosion in Urbanizing Watersheds of Ghana: Implications for Watershed Management. *Environmental Management*, **61**, 659-671.

[29] Ouattara, K., Kouassi, A.M. and Srohourou, B. (2017) Evaluation of Soil Erosion in Rural Watersheds of Central Côte d'Ivoire Using RUSLE Model and GIS. *International Journal of Scientific & Technology Research*, **6**, 123-130.

[30] Adamou, S.N., Gourfi, A., Touré, A.A. and Daoudi, L. (2022) Érosion hydrique au sud-ouest du Niger: Impacts des facteurs naturels et anthropiques sur les pertes en sols. Géomorphologie. *Relief*, *Processus*, *Environnement*, **28**, 77-92. https://doi.org/10.4000/geomorphologie.16744

[31] FAO and ITPS (2015) Status of the World's Soil Resources (SWSR) Main Report. Food and Agriculture Organization of the United Nations and Intergovernmental Technical Panel on Soils, Rome, Italy. http://www.fao.org/3/a-i5199e.pdf

[32] Kouadio, K.A., Koffi, B. and Konan, B.K. (2021) Impact of Urbanization on Surface Runoff and Soil Erosion in Abidjan (Côte d'Ivoire): A Remote Sensing and GIS Approach. *Journal of Geoscience and Environment Protection*, **9**, 1-18.